Study of the contribution of different effects induced by the punching process on the high cycle fatigue strength of the M330-35A electrical steel

Helmi Dehmani [a,b,c]* Charles Brugger[b], Thierry Palin-Luc[b], Charles Mareau[c], Samuel Koechlin[a]

[a]*Leroy Somer, Boulevard Marcellin Leroy 16915 Angoulème, France*
[b]*Arts et Métiers ParisTech, I2M, CNRS, Esplanade des Arts et Métiers, 33405 Talence – France*
[c]*Arts et Métiers ParisTech, LAMPA, 2 boulevard du Ronceray, 49035 Angers – France*

Abstract

Because of their improved magnetic properties, Fe-Si alloys are widely used for new electric motor generations. The use of punching process to obtain these components specially affects their mechanical behavior and fatigue strength. This work aims at studying the influence of punching operations on the fatigue behavior of a Fe-Si alloy. High cycle fatigue tests are performed on different smooth specimen configurations with either punched or polished edges. Results show a significant decrease of the fatigue strength for punched specimens compared to polished ones. To understand the origin of the fatigue failure on punched specimens, SEM observations of the fracture surfaces are carried out. They reveal that crack initiation always occurs on a punch defect. Additional experimental techniques are combined to characterize how the edges are altered by punching. The impact of punching operations on residual stresses and hardening is then investigated. Residual stresses are quantified on punched edges using X-ray diffraction techniques. Important tensile residual stresses exist in the loading direction as a result of punching operations. Also, according to XRD analyses and micro-hardness measurements, the hardened zone depth is about 200 µm. To dissociate the respective influences of strain hardening, residual stresses and geometrical defects, a heat treatment is applied to both punched and polished specimens in order to quantify the contribution of each parameter to the high cycle fatigue resistance. Results show that the geometry of defects is one of the most influent parameters. Consequently, a finite element model is developed to simulate the influence of edge defects on the fatigue strength of punched components. A non-local high cycle fatigue criterion is finally used as post-processing of FEA to consider the effect of defects and the associated stress-strain gradients in the HCF strength assessment.

Keywords: Electrical steel, high cycle fatigue, punching effect, defect, residual stress

1. Introduction

Thin electrical steel sheets are widely used in the building of electric motors because of their improved magnetic properties. To increase efficiency, material suppliers have developed new electric steel grades with reduced iron losses. The magnetic properties improvement is achieved by adjusting the chemical composition (mainly the silicon content), reducing the thickness below 0.5 mm and increasing the grain size. The punching process is widely used for sheet metal working because it offers high production rates and low costs. It however significantly influences the durability of components, mostly because important alterations of edges are usually observed. More specifically, punching operations generate a specific morphology on edges with different characteristic zones: roll over, shear zone, fracture zone and burr. The dimensions of each zone depend on the sheet thickness and the punch tool clearance [Baudouin et al. (2003)]. In addition to this morphology, the punching process generates important alterations of the sheet edges such as hardening, tensile residual stresses and geometrical defects [Achouri et al. (2014), Lara et al. (2013), Sanchez et al. (2004), Maurel et al. (2003)]. As a result of the aforementioned alterations, the punching process is responsible for the degradation of the high cycle fatigue resistance of punched components. Sanchez et al. (2004) carried out fatigue tests on flat specimens (with 15 mm thickness) made in bainitic and ferritic–pearlitic steels. In order to study the effect of the process on the fatigue resistance, the authors compared test results of specimens with either punched or drilled holes. An important decrease of the fatigue resistance is observed for punched specimens. Also, Lara et al. (2013) performed fatigue tests on specimens obtained with different techniques: laser cutting, punching, punching then polishing. Results show that fatigue properties of punched specimens are the lowest. SEM observations of fracture surfaces reveal that crack initiation occurs on edges, on defects generated during punching operations. However, for polished specimens, initiation occurs no longer on the edge but either on inclusions resulting from material elaboration or from surface defects caused by rolling process. In order to investigate the origin of the fatigue strength drop in the case of punched specimens, micro-hardness measurements have been performed by Ossart el al. (2000) on a punched electrical steel sheet with a thickness of 0.5 mm. Measurements were done starting from the punched edge. Results show an important gradient of the mechanical properties and the hardened layer depth which is generated by the punching operation.

The objective of this paper is to quantify the contribution of the following effects: hardening, residuals stresses and geometrical defects (all induced by punching) to the high cycle fatigue resistance drop of an iron-silicon alloy used for building electric motors.

2. Experimental procedure

The studied material is M330-35A electrical steel delivered in the form of rolled sheets with a nominal thickness of 350 μm. Metallographic observations reveal an equiaxed microstructure with a mean grain size of 100 μm (Fig. 1a). Monotonic tensile tests have been performed on specimens obtained from three different directions in the sheet plane. Results show that the maximal difference for the yield stress is about 7%. As a consequence, in the following, mechanical properties are considered to be isotropic. High cycle fatigue tests have been performed in air under uniaxial tension loading along the rolling direction, using a resonant fatigue testing machine (Vibrophore type) at a frequency of 64 Hz. Tests were carried out on smooth specimens (Fig. 1b) at room temperature (≃20°C) using R=0.1 loading ratio. A parallel edge geometry with a calibrated zone was used for fatigue tests. It allows cut edge defects to be critical whatever their position along the 20 mm gauge length. The stop criterion was a frequency drop of 1 Hz, which corresponds to the total specimen's failure, or when the maximum number of cycles (5×10^6 cycles) was reached. In order to quantify the contribution of each effect induced by the punching process on the fatigue resistance of this Fe−Si alloy, different specimen configurations were tested:

- (C1) Punched specimens
- (C2) Punched then polished specimens
- (C3) Punched then annealed specimens
- (C4) Punched then polished then annealed specimens

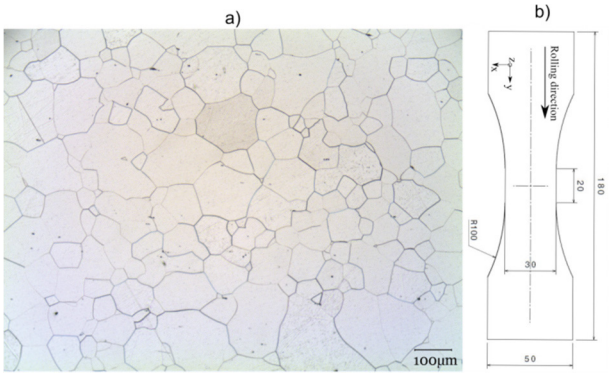

Fig. 1. (a) Fe-Si alloy microstructure (b) fatigue specimen geometry

Mechanical polishing was done using silicon carbide papers from P1200 to P4000 grades until all visible defects were removed. Polishing operations are expected to modify the hardening and the residual stress distribution initially induced by punching. Moreover, in order to relieve residual stresses and eliminate hardening induced by punching, an annealing treatment was applied to some specimens in a controlled environment. As a consequence of this treatment, a local recrystallized region, which is about 50 µm deep, is observed for punched and annealed specimens. In this region, the initial large grains (Fig. 2a) are thus transformed into small grains with no hardening (Fig. 2b).

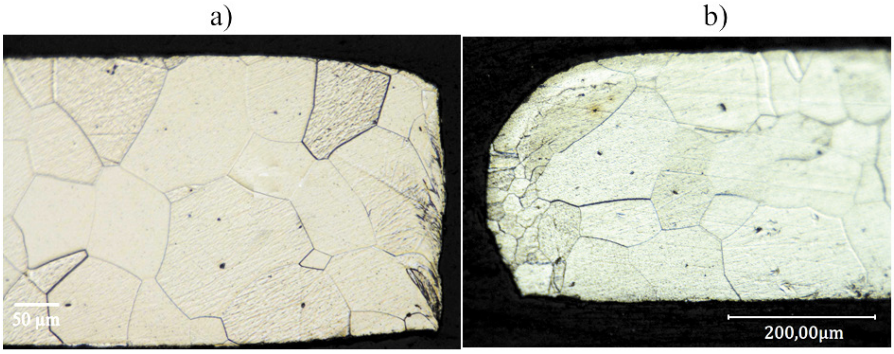

Fig. 2. (a) Punched edge with large grains and hardening (b) punched edge after annealing with local recrystallization

3. Fatigue tests results

3.1. S−N curves

The S–N curves corresponding to the different specimen configurations are presented in Fig. 3a. The fatigue strength has been estimated using the staircase method. To quantify the contribution of the different effects induced by the punching process, the punched−polished−annealed configuration (C4) is taken as reference (see Table1). All the effects of the punching process are related to C1 specimens. Results show a drop of 20% on the median fatigue strength at 5×10^6 cycles. The effect of punching defects (geometric effect only) is then investigated. A drop of 8% is observed in the case of C3 specimens. But an increase of 11% of the fatigue resistance is observed for C2 specimens. This represents the positive effect of the mechanical polishing process. However, for high stress levels, the difference between the different configurations is reduced since fatigue crack initiation is governed by the macroscopic plasticity of the specimen. To investigate the causes of these differences, the following techniques have been used: microscopic observations, X-ray diffraction and micro-hardness measurements.

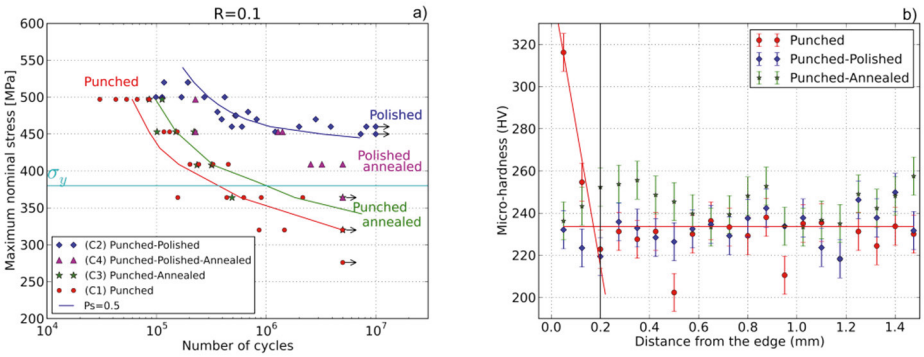

Fig. 3. (a) S-N curves obtained for different specimen's configurations, (b) Micro-hardness measurements for different specimen's configurations (vertical bars represent experimental uncertainty)

Table 1. Median values of fatigue strength for different specimen's configurations.

Configuration	σ_D [MPa]	Standard deviation [MPa]	Difference (%)
C4: Punched−polished−annealed	184	20	0 (reference)
C3: Punched−annealed	169	20	– 8
C2: Punched−polished	204	20	+ 11
C1: Punched	147	20	– 20

3.2. Fractographic observations

To explain the differences between the different configurations and to identify the crack initiation mechanisms, SEM observations of fracture surfaces have been performed. For punched (C1), and punched−annealed specimens (C3), initiation occurs on a punching defect located, in most cases, in the fracture zone (Fig. 4a). On the contrary, for punched−polished specimens (C2), initiation is transgranular (Fig. 4b). Since initiation mechanisms depend on the nature of the edge (either punched or polished), there is an important influence of the process on fatigue crack initiation.

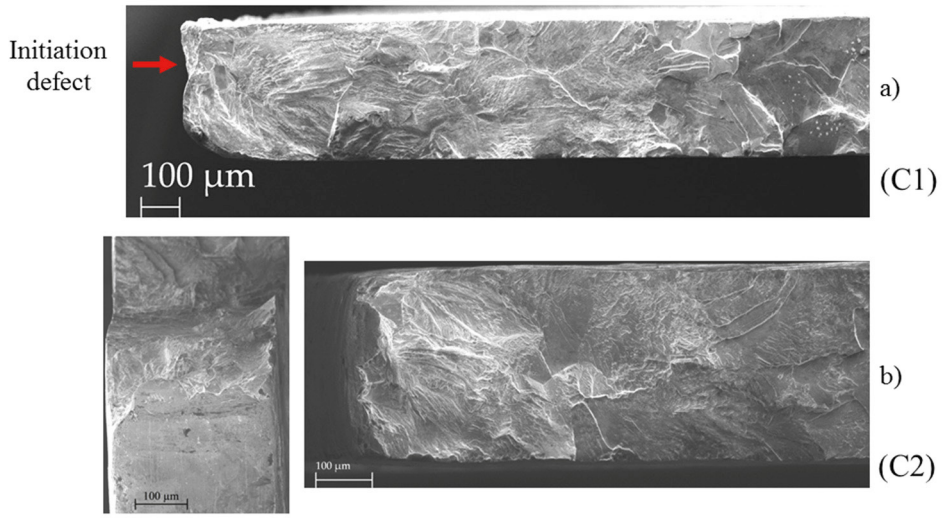

Fig. 4. SEM observations of fracture surfaces (a) punched specimens (C1), (b) punched-polished specimens (C2)

4. Discussion

4.1. Micro-hardness measurements

To determine the depth of the layer affected by punching and polishing operations, micro-hardness measurements (HV 0.1) were performed on some specimens from the C1, C2 and C3 configurations. The first indentation was located 50 µm from the edge, the subsequent indentations were spaced with 75 µm to avoid measurement interferences. Results presented in Fig. 3b show that the hardening layer depth is about 200 µm. Moreover, to verify that hardening is eliminated by the annealing treatment, micro-hardness measurements are performed on C3 specimens. On these specimens, hardening is eliminated by the heat treatment and micro-hardness values are close to the polished specimens.

4.2. XRD analyses

X-ray diffraction techniques offer a better resolution for estimating the hardened depth. In the present work, because of the low sheet thickness, analyses were performed on a stack of 10 sheets. Each stress value was estimated on an irradiated zone which approximately corresponds to a 2 mm diameter disk. Residual stresses were determined first on punched edges, then on surfaces obtained after successive layer removal operations using electrochemical polishing techniques. Analyses were conducted for C1, C2 and C3 specimens. The results relative to the in-depth evolution of longitudinal residual stresses σ_{yy} are presented in Fig. 5a. Punched specimens exhibit high tensile residual stresses. However, for punched−polished specimens, important compression residual stresses exist on edges. For punched−annealed specimens, residual stress analyses were performed only on edges (zero depth). Results show that the high tensile residual stresses initially induced by punching are fully relieved after the annealing treatment. The Full Width at Half Maximum (FWHM) provides a qualitative evaluation of hardening. The evolution of the FWHM, associated with X-ray analyses, as a function of depth is plotted for C1, C2 and C3 specimens in Fig. 5b. The maximum value is obtained on the top surface of the edge, then values decrease and stabilize with an increasing depth. For punched specimens, the results show that the depth affected by punching operations is about 200 µm, which is consistent with micro-hardness measurements.

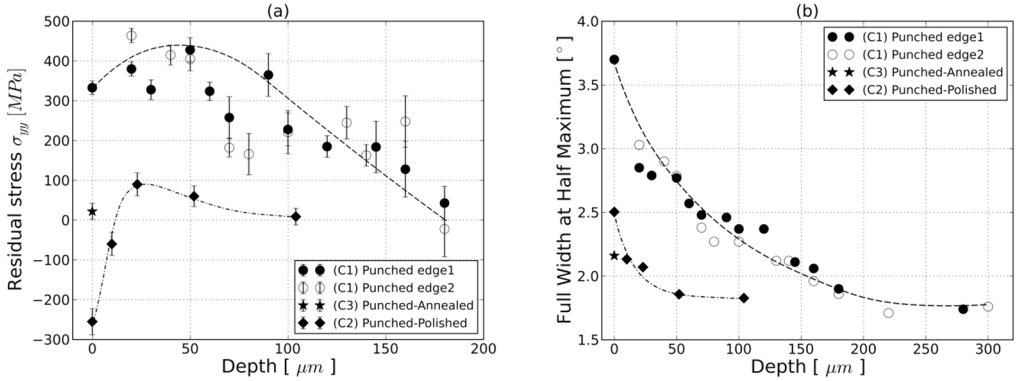

Fig. 5. (a) Longitudinal residual stress σ_{yy} profile for punched, punched-polished and punched-annealed specimens (b) Full Width at Half Maximum relative to X-ray analyses

4.3. Punching defects

Punched edges have been examined using microscopic observations and an optical profilometer. The scanned zones contain the entire reduced section and a part of the specimen radius. The resolution used for scanning surface edges is 0.89 µm along the X and Y directions and 10 nm along the Z direction. Results show an irregular edge surface

with four types of defects (see Fig.6): (i) vertical stripes from the top to the bottom of the edge, (ii) depressions in the top surface (roll-over defects), (iii) defects in the sheared zone, (iv) defects in the fracture zone. The most harmful defects are located in the fracture zone with typical dimensions (about 60 µm) close to those of a grain. This confirms SEM observations about the criticity of punching-induced defects.

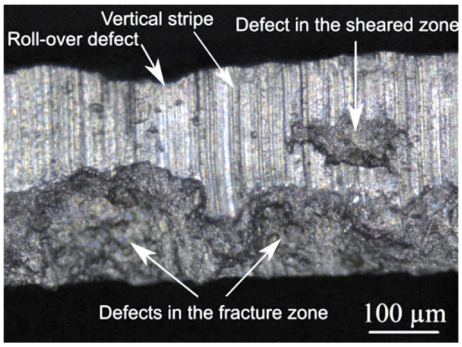

Fig. 6. Different types of defect in the punched edge

From three dimensional surface topography data, the linear density of punching defects was determined, the Murakami parameter ($\sqrt{area}$) has then been adopted to define the defect size [Murakami (2002)]. The shear zone is considered as reference to determine the defect area (see Fig. 7a). Observations have been performed on about 650 mm length of punched edges. The mean value of the defect size is 56 µm. The distribution of the largest defects (with $\sqrt{\text{area}} > 56$ µm) located in the fracture zone is presented in the histogram plotted in Fig. 7b. Results show that biggest defect sizes are mainly between 60 µm and 70 µm. However, there are some defects with a size larger than 80 µm.

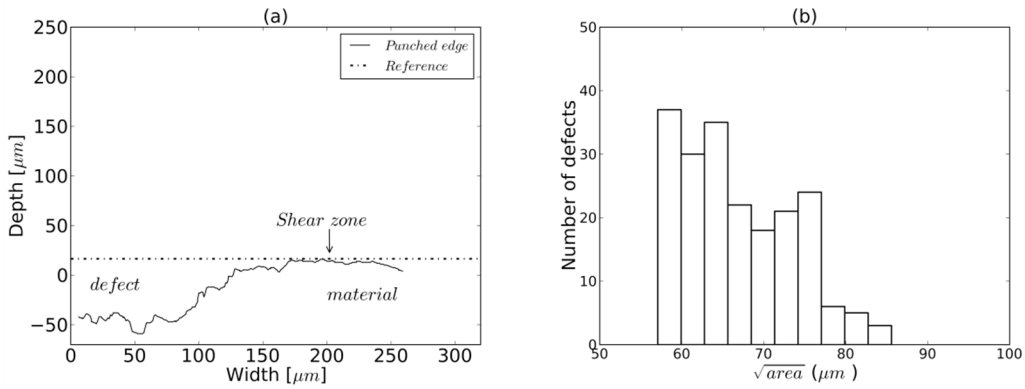

Fig. 7. (a) Reference for critical defect size calculation, (b) distribution of largest punching defects

In order to determine if the size or the shape of the defect is the most important parameter for fatigue crack initiation, finite elements analyses (FEA) were performed on punching defects obtained from three dimensional surface topography data. The adopted strategy to identify the critical defect and to get its geometry is detailed in Dehmani et al. (2016).

5. FEA of the notch effect of punching defects

To propose a fatigue design strategy for punched components, Crossland local and volumetric approaches were evaluated in post-processing of FEA. The developed model considers the geometrical effect of punching defects. Moreover, the residual stresses are taken into account when calculating the criterion threshold.

In order to determine the stresses and strains distributions around the critical defects, FEA were performed on real defect geometries. The boundary conditions used for the simulations are illustrated in Fig. 8. To ensure the mesh convergence and to optimize the simulation time, a mesh dimension sensitivity study was performed. An element size of 5 µm along the X and Y directions and 10 µm in along the Z direction was finally chosen. Simulations were performed using either an elastic or an elastic-plastic constitutive model. For the elastic-plastic behavior, a linear isotropic hardening rule was used to describe the evolution of the yield surface. The material model parameters were identified from the results of low cycle fatigue tests carried out on the studied alloy under load control (like in the high cycle fatigue tests).

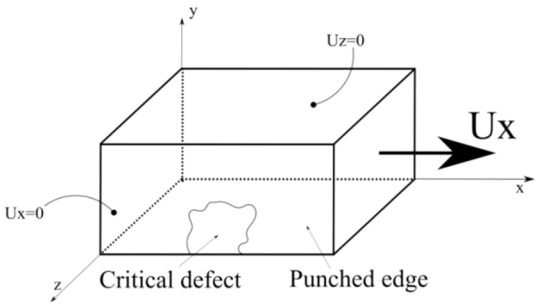

Fig. 8. Boundary conditions used for the FE simulations

Local [Crossland (1956)]and non-local (volumetric) formulations [ElMay et al. (2015)] of the Crossland high cycle multiaxial fatigue criterion were used for post-processing the results of FEA. The threshold relative to C4 specimens, which represents the material without any influence of the process, is used for evaluating the Crossland criterion. For the volumetric approach, the critical distance d_c was optimized on one critical defect geometry (the same for elastic and elastic-plastic calculations) in order to have an averaged danger coefficient close to 1. The averaging distance was optimized at 55 µm and 45 µm for elastic and elastic-plastic calculations respectively. Since fatigue tests were conducted in the high cycle regime, the applied stress levels (for R=0.1 loading ratio) are less than the material yield stress. Moreover, punching process induces hardening near the edges, so one can assume that the material behavior is still elastic in all specimen's regions. This assumption was verified through XRD analyses performed by Dehmani et al. (2016) on specimens tested at R=0.1 loading ratio. In comparison with the initial residual stress state, no significant redistribution was observed for these loading conditions. Consequently, punching-induced local hardening seems to prevent cyclic plasticity to occur on the edges. However, since analyses were performed on a stack of 10 specimens, the measured residual stresses are averaged values. Since the used experimental technique has not sufficient spatial resolution to reliably determine if there is plasticity near the edge defect, the adopted FEA strategy allows to study the two possible cases. The points representing the shear stress amplitude versus the maximal hydrostatic stress calculated at the integration points of the FE model are plotted in the Crossland diagram (Fig. 9) for a critical defect. Points are calculated using the local and the volumetric Crossland approaches. Results show that the local approach does not lead to safe fatigue strength assessment because many points are located in the criterion failure zone. The volumetric approach gives better results. However, this approach was verified only for two critical defect geometries. It should therefore be verified using other critical defects. Since the developed FE model only considers the geometrical effect of punching defects, the residual stresses are taken into account when calculating the criterion threshold. The effect of residual stresses can be simply added for elastic calculations. However, for elastic-plastic calculations, it is not theoretically correct to

add residual stresses effect. The introduction of residual stresses distribution in the model is very difficult and it is proposed as prospect of this work.

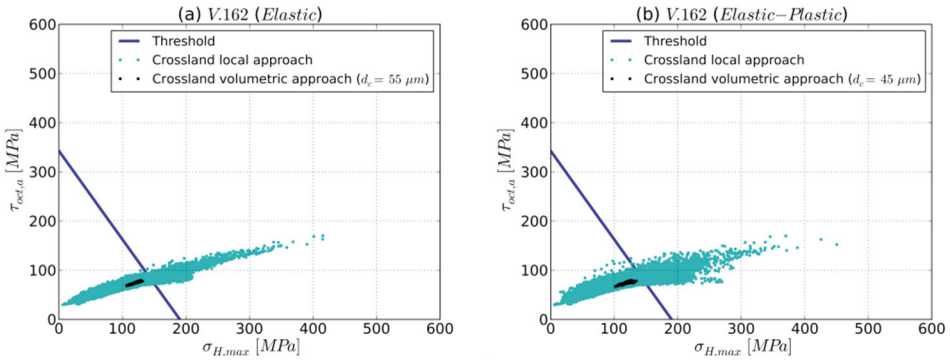

Fig. 9. Comparison between local and non-local Crossland diagram formulations for an identified critical defect

6. Conclusion

In this paper, the effect of the punching process on the high cycle fatigue resistance of thin Fe-3%Si steel sheets was investigated. Fatigue tests performed on different specimen configurations allowed for quantifying the contribution of different effects: hardening, residual stresses and geometrical defects on the fatigue resistance of the studied alloy. Results show that the punching process is responsible for a 20% drop of the median fatigue strength at 5×10^6 cycles. The drop due to the geometrical defects is about 8%. Investigations were carried out on different specimen edges. XRD analyses reveal that high tensile residual stresses exist locally on the punched edges. Micro-hardness and XRD measurements near cut edges show that the depth of the mechanically affected zone is about 200 µm. Finite element analyses were conducted on critical defect geometries obtained from three dimensional surface topography. The Crossland multiaxial fatigue criterion with its local and non-local formulations was used for the post-processing of FEA. Results show that Crossland local approach does not lead to safe fatigue strength assessment. However, the non-local formulation gives better results. Since the Crossland volumetric approach was evaluated only for two defects, simulations on other critical defect geometries are needed to confirm the proposed methodology. Additional work is needed to take into account the effect of the field of residual stresses on the HCF strength.

References

Baudouin, P., Wulf, M. De, Kestens, L., Houbaert, Y., 2003. The effect of the guillotine clearance on the magnetic properties of electrical steels, Journal of Magnetism and Magnetic Materials, 32–40, 256

Achouri, M., Gildemyn, E., Germain, G., Dal Santo, P., Potiron A., 2014. Influence of the edge rounding process on the behaviour of blanked parts: numerical predictions with experimental correlation, Int J Adv Manuf Technol., 71(5-8).

Lara, A., Picas, I., Casellas, D., 2013. Effect of the cutting process on the fatigue behaviour of press hardened and high strength dual phase steels. Journal of Materials Processing Technology, 1908– 1919.

Sanchez, L., Gutierrez-Solana, F., Pesquera, D., 2004. Fatigue behaviour of punched structural plates. Engineering Failure Analysis, 751–764.

Maurel, V., Ossart, F., Billardon, R., 2003. Residual stresses in punched laminations: Phenomenological analysis. Journal of Applied Physics 93, 7106.

Florence, O., 2000. Dégradation du comportement magnétique des tôles lors de leur mise en œuvre industrielle : mise en évidence expérimentale et modélisation, Mécanique & Industries, 1(2), 165–176.

Murakami, Y., 2002. Metal fatigue: effect of small defects and non-metallic inclusions, Elsevier Ed., 369.

Dehmani, H., Brugger, C., Palin-Luc, T., Mareau, C., Koechlin, S., 2016. Experimental study of the impact of punching operations on the high cycle fatigue strength of Fe–Si thin sheets, International Journal of Fatigue, 82, 721–729.

Crossland. B., 1956. Effect of large hydrostatic pressures on the torsional fatigue strength of an alloy steel, Proc. Int. Conf. on Fatigue of Metals, 138.

ElMay, M., Saintier, N., Palin-Luc T., Devos, O., 2015. Non-local high cycle fatigue strength criterion for metallic materials with corrosion defects. Fatigue Fract Engng Mater Struct, 38, 1017–1025.